Nanoparticle Based Printed Sensors on Paper for Detecting Chemical Species

Jack Lombardi, Mark D. Poliks*
Department of System Science and Industrial Engineering
State University of New York at Binghamton
Binghamton, NY, USA
jlombar4@binghamton.edu, mpoliks@binghamton.edu

Ziang Pan
Materials Science & Engineering Program*
State University of New York at Binghamton
Binghamton, NY, USA

Wei Zhao, Shan Yan, Ning Kang, Jing Li, Jin Luo, Chuan-Jian Zhong
Department of Chemistry
State University of New York at Binghamton
Binghamton, NY, USA

Mihdhar Almihdhar, Benjamin S. Hsiao
Department of Chemistry
State University of New York at Stony Brook
Stony Brook, NY, USA

Madina L. Zabran, Sandeep S. Mittal, Kanad Ghose
Department of Computer Science
State University of New York at Binghamton
Binghamton, NY, USA

Abstract— **There has been an increasing need of technologies to manufacturing chemical and biological sensors for various applications ranging from environmental monitoring to human health monitoring. Currently, manufacturing of most chemical and biological sensors relies on a variety of standard microfabrication techniques, such as physical vapor deposition and photolithography, and materials such as metals and semiconductors. Though functional, they are hampered by high cost materials, rigid substrates, and limited surface area. Paper based sensors offer an intriguing alternative that is low cost, mechanically flexible, has the inherent ability to filter and separate analytes, and offers a high surface area, permeable framework advantageous to liquid and vapor sensing. However, a major drawback is that standard microfabrication techniques cannot be used in paper sensor fabrication. To fabricate sensors on paper, low temperature additive techniques must be used, which will require new manufacturing processes and advanced functional materials.**

In this work, we focus on using aerosol jet printing as a high-resolution additive process for the deposition of ink materials to be used in paper-based sensors. This technique can use a wide variety of materials with different viscosities, including materials with high porosity and particles inherent to paper. One area of our efforts involves creating interdigitated microelectrodes on paper in a one-step process using commercially available silver nanoparticle and carbon black based conductive inks. Another area involves use of specialized filter papers as substrates, such as multi-layered fibrous membrane paper consisting of a poly(acrylonitrile) nanofibrous layer and a nonwoven poly(ethylene terephthalate) layer. The poly(acrylonitrile) nanofibrous layer are dense and smooth enough to allow for high resolution aerosol jet printing. With additively fabricated electrodes on the paper, molecularly-functionalized metal nanoparticles are deposited by molecularly-mediated assembling, drop casting, and printing (sensing and electrode materials), allowing full functionalization of the paper, and producing sensor devices with high surface area. These sensors, depending on the electrode configuration, are used for detection of chemical and biological species in vapor phase, such as water vapor and volatile organic compounds, making them applicable to human performance monitoring. These paper based sensors are shown to display an enhancement in sensitivity, as compared to control devices fabricated on non-porous polyimide substrates. These results have demonstrated the feasibility of paper-based printed devices towards manufacturing of a fully wearable, highly-sensitive, and wireless human performance monitor coupled to flexible electronics with the capability to communicate wirelessly to a smartphone or other electronics for data logging and analysis.

Keywords-sensor packaging; disposable; emerging materials; flexible electronics; wearable and medical electronics; novel materials and processing

I. INTRODUCTION

Paper-based sensors have shown increasing promises as low-cost, portable and disposable sensor devices for a wide range of applications, including wearable sensors, biosensors, clinical diagnosis, food quality control and environmental monitoring [1]–[4]. These sensors often have properties and performance that are superior to those made on conventional sensor materials. Examples include simplicity of processing and fabrication, passive liquid transport and compatibility with chemicals/biochemicals.

2377-5726/17 $31.00 © 2017 IEEE
DOI 10.1109/ECTC.2017.320

While paper sensors have clear advantages in terms of sensing performance and materials cost, the integration of paper into electronic circuitry to transduce and communicate remains to be a challenging area. This work aims to show how printed paper sensors can be effective for detecting chemical species, and could be mated to hybrid flexible electronics to create hybrid flexible sensors. One area of active research involves printing functional electrodes onto paper-based platforms using different conductive inks. For example, using carbon or silver inks, printed electrodes on paper were shown to be viable for the detection of glucose, lactate and uric acid [5]. The conductive electrode pads were screen-printed in the hydrophilic region of the paper where enzymes were subsequently spotted, and changes in electrical conductivity in the presence of a chemical species provided sensing signals. There are also examples using the paper-based sensing in the gas-phase [6], [7]. Arena et al [6] reported a paper-based sensor for ethanol detection, in which the sensing layer was fabricated on multi-walled carbon nanotube based electrodes with indium tin oxide particles using poly-diallyldimethylammonium chloride as the binder. Steffens et al [7] developed a gas sensor on paper in which graphite interdigitated electrodes were coated with a thin film of doped-polyaniline as the sensing electrodes.

While there has been research demonstrating the viability of 2D sensing materials on paper, few have explored the 3D framework and structure of paper in constructing sensors. Herein we report a novel class of nanocomposite sensor fabricated by printing a silver or carbon ink onto nanofibrous membrane and assembling gold nanoparticles in it to create a chemiresistor. The nanofibrous membrane consists of two-layered structures, including cross-linked polyacrylonitrile (PAN) and polyethyleneterephthalate (PET) fibrous layer [8]. A molecularly-mediated thin film of gold nanoparticles assembled via hydrogen-bonding is embedded in the membrane as sensing materials [9]. The sensing platform couples the nanoparticle thin film's tunable molecular interactions and electrical properties with the nanofibrous membranes featuring a high surface-to-volume ratio [8], [9]. This strategy is expected not only to enhance the sensor performance but also further widen the sensor applications.

While the creation of a chemiresistive sensor in paper is useful, there are technical challenges to enable its wearable application. Electronics and packaging must be added to create a useful, wearable sensor system, with a power supply, signal conditioning and sensing, wireless communication and microprocessor. Researchers have successfully created this type of flexible electronic sensor system. In the work by Imani et al [10], a system with combined electrical, chemical and physiological sensors was demonstrated using screen printing to create electrodes on a flexible 50μm thick polyester sheet. These electrodes were interfaced to a flexible printed circuit board for data collection and transmission via Bluetooth radio. This sensor was able to produce an electrocardiogram as well as sense the presence of lactate in the sweat [10]. Gao at al [11] was also able to use flexible printed circuit board technology to make a wearable sensor for detecting glucose, lactate, sodium and potassium ions in sweat, as well as temperature. This flexible sensor could then be wrapped around a person as a smart headband or bracelet, and transmit physiological data via Bluetooth radio [11].

For a wearable application, the sensor components should be packaged in a way to give a small, flexible system compatible with the printed paper device, and amenable to the single use, disposable nature of the paper. To do this we leverage an existing flexible electronic system, a hybrid flexible electronic human performance monitor (HPM), that has these components and functions already established as part of previous work [12], [13]. This sensor has demonstrated high quality electrocardiograms (ECG), temperature sensing, and wireless communication, and has the capacity to be linked to a paper sensor with minimal modification. This device has existing voltage supplies, analog channels, and connection points for screen printed devices which could be used with minimal modification to the original HPM.

Overall, we will show how nanoparticle sensitized chemiresistive sensors can be fabricated on paper using AJP, the increase in sensor performance due to the use of paper substrates, and the feasibility of integrating these sensors onto existing hybrid flexible HPM to create flexible/wearable chemical sensors.

II. Experiments and Materials

A. Chemicals and Materials

Chemicals and Materials. Hydrogen tetrachloroaurate trihydrate (99%), tetraoctylammonium bromide (99%), decanethiol (DT, 96%), sodium borohydride (99%), 11-mercaptoundecanoic acid (MUA, 95%) were purchased from Aldrich. Solvents included hexane (Hx, 99.9%)，toluene (Tl, 99%), and benzene (Bz, 99.0%) from Fisher, and ethanol (99.9%) from Aldrich. Water was purified with a Millipore Milli-Q water system. The silver ink used was Paru PG-007, which consists of ethylene glycol and 1-methoxy-2-propanal based components mixed in a weight ratio of 1:5. The carbon black based ink was Methode Electronics 3804 aqueous ink, which was diluted 1:1 by volume to enhance printing. Tetramethylpiperidinooxy (TEMPO, 98 %) was purchased from Acros. Sodium hypochlorite (NaClO solution, available chlorine 7 ~ 10 %) was purchased from Sigma-Aldrich. Sodium bromide (NaBr) was obtained from Fisher Scientific Company. Polyacrylonitrile (PAN) having a weight-average molecular weight of 150kDa was purchased from Sigma-Aldrich. Poly (ethylene terephthalate) non-woven substrate (PET microfilter FO2413 with an average fiber diameter of about 30 μm) for the membrane support was provided by Freudenberg Nonwovens (Hopkinsville, KY). UPILEX-25S polyimide film was also used as a substrate for printing.

B. Nanoparticle Synthesis

Gold nanoparticles of 2nm diameter (Au_{2nm}) encapsulated with decanethiolate monolayer shells were synthesized by two-phase reduction of $AuCl_4^-$ according to Brust's two-phase protocol and a synthetic modification [14]. The as-synthesized gold nanoparticles (DT-Au_{2nm}) exhibited an average size of 2.0±0.7nm. DT-capped gold

nanoparticles with larger sizes were synthesized by a thermally-activated processing route developed in our laboratory [15]. Briefly, the solution containing the as-synthesized DT-Au_{2nm} nanoparticles was heated at 150°C to develop larger-sized Au nanoparticles. Gold nanoparticles of 7.0±0.5nm diameters (Au_{7nm}) produced by this method were used in this work.

C. Preparation of Nanofibrous Membranes

PAN was dissolved in DMF at 60°C for 2 days until the mixture became a homogeneous solution (the solution concentration was 8 wt%). The homogeneous PAN solution was electrospun onto the non-woven PET substrate under a high electrical voltage of 20kV. The flow rate during this electrospinning operation was 16μL/min and the inner diameter of the spinneret was 0.7mm. The working distance between the spinneret and the collector was 10cm. The mean fiber diameter of the electrospun nanofiber estimated from the SEM image was 150±10nm.

D. Preparation of Thin Film Assemblies of Nanoparticles

Thin film assembly of MUA linked DT-capped Au NPs were prepared via an "exchanging-crosslinking-precipitation" route with a controlled 50-500 ratio of MUA to Au nanoparticles [16]. The reaction involved an exchange of linker molecules MUA with the gold-bound alkanethiolates, followed by crosslinking and precipitation via Au-S bonding at one end of MUA and hydrogen bonding at the carboxylic acid terminals of MUA. For MUA-Au films, stock solutions of DT-capped Au (5nm) (~30μM) in hexane and MUA (10mM) in ethanol were used. The silver ink printed microelectrodes on the paper membrane and polyimide substrates were immersed into the solution, and let it sit for overnight.

E. Sensor Measurements

A computer-interfaced multi-channel meter (Keithley, Model 2700) was used to measure the lateral resistance of the nanostructured thin films on the chemiresistor devices, which were housed in a Teflon chamber with tubing connections to vapor and N_2 sources. All experiments were performed at room temperature, 22±1°C. N_2 gas (99.99%, Airgas) was used as reference gas and as diluent to change vapor concentration by controlling mixing ratio. The vapor concentration was controlled by a flow-control system, bubbling dry N_2 gas through a selected vapor solvent. The gas flow was controlled by a calibrated Aalborg mass-flow controller (AFC-2600). The flow rates of the vapor stream were varied between 3 and 99mL/min, with N_2 added to a total of 100mL/min. The vapor generating system consisted of multi-channel module linked to different vapor sources. The modular platform components permitted different vapor flow with minimum dead-volume and virtually no cross-contamination. The test chamber was purged with pure nitrogen to establish the baseline before introducing analyte vapor. The vapor concentration in the unit of ppm as a molar ratio was determined from the partial vapor pressure and the mixing ratio of vapor and N_2 flows, which can be converted to ppm as a volume ratio, necessary for vapor concentration measurements, by multiplying a factor of 24.5 [17]. The measured resistance (R_Ω) is related to the lateral conductivity (σ) of the film [18]. ΔR is the difference of the maximum and minimum values of the resistance in response to vapor exposure, and R_i is the initial resistance of the film. The response sensitivity was determined from the relative differential resistance change, $\Delta R/R_i$, versus vapor concentration, C (ppm) for the evaluation of the vapor sorption responses.

Measurements were also made with a TI CC2650 evaluation module to evaluate the feasibility of using the printed sensor on the HPM. This module allows for the use and testing of the CC2650 microcontroller, which is used in the HPM, without needing an actual HPM, and also allowing easier interfacing and control with a computer. In this test, the 12 bit analog to digital converter of the module was used to sense the voltage across a voltage divider created with a printed sensor. A 1MΩ resistor was used as part of the voltage divider, powered by a 3V battery pack, emulating the 3V available on the actual HPM. A digital value could then be observed on the evaluation module corresponding to the observed voltage and indicating a change in the resistance of the sensor.

F. Device Fabrication

Fabrication of all devices started with the printing of the interdigitated microelectrodes (IME) using an Optomec AJ-300 aerosol jet printer. Two different materials and designs were used, and each will be described. Interdigitated silver microelectrodes were printed on the paper membrane using the Paru silver ink in the pneumatic atomizer and a 200μm tip. A print speed of 10mm/s was used and lines of 140μm were produced. The electrodes consist of 20 fingers 3mm long at 140μm spacing bordered by 1mm wide traces. Two layers were printed on each electrode. Following printing, the electrodes were left to dry in air at room temperature before being sensitized. Interdigitated carbon electrodes were printed using the diluted Methode ink in the ultrasonic atomizer and a 150μm tip. A print speed of 10mm/s was used and lines of 40μm were produced. The electrodes consist of 30 fingers which are 1.27mm long, at 40μm spacing, with 1.27mm wide traces on each side. Two layers were printed on each electrode. Printed electrodes were baked in an oven at 50 for one hour following printing to increase conductivity.

III. Results and Discussion

A. Morphologies of Nanocomposite Paper Sensors

Fig. 1 shows a set of schemes, photos and SEM images to illustrate the coupling of Au nanoparticles as sensing materials with Ag-printed IME on paper membranes (PAN/PET) as a sensor platform [19]. The 2-layer paper (PAN/PET) was used as the substrate for constructing the sensors. The Ag IME were printed on the top of the PAN layer by Aerosol inkjet printer at room temperature. The MUA-linked Au nanoparticles were assembled into the PAN layer, as shown in Fig. 1(a)-(c) via a combination of hydrogen-bonding and van der Waals interactions of the

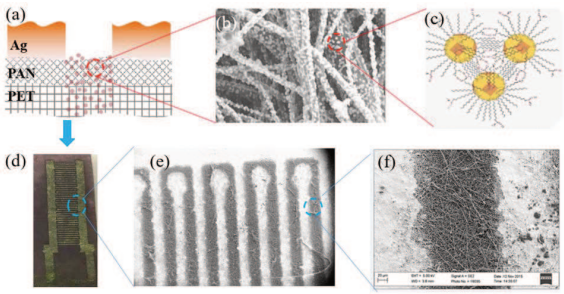

Figure 1. (a) Scheme showing Au nanoparticles as sensing materials coupled with Ag-printed IME on paper membranes (PAN/PET) as a sensor platform. (b) SEM image of MUA-Au assembled on PAN fibers. (c) Scheme of the molecular interactions in the assembly of Au nanoparticles by MUA as linkers. (d) Photo showing an Ag-IME/ PAN/PET paper membrane device with MUA-Au thin film. (e) and (f) SEM images showing the magnified views of the Ag-printed IME on PAN/PET paper membrane.

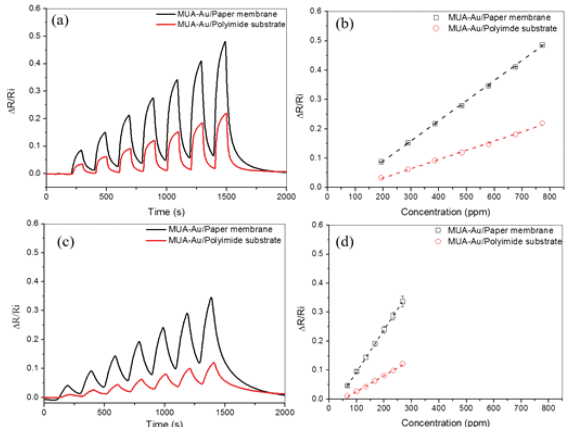

Figure 2. Response profiles to VOCs for a MUA-linked Au nanoparticle thin film as sensing materials on PAN/PET paper membrane (black) based Ag interdigitated microelectrodes device. Data for printed Ag IME on polyimide substrate (red) are included for comparison. (a) Ethanol with concentrations from 200 to 800 ppm. (b) Plot of ethanol response and linear fit, showing slope of 6.87×10^{-4} and 3.15×10^{-4} for paper and polyimide substrates, respectively. (c) 1-propanol with concentrations from 50 to 275 ppm (d) Plot of 1-propanol response and linear fit, showing slope of 1.45×10^{-3} and 5.49×10^{-4} for paper and polyimide substrates, respectively.

MUA and DT on the Au nanoparticles. After thin film assembly, the color of the membrane changes from white to purple, as shown in Fig. 1(d), indicating the incorporation of the nanoparticle thin films in the membrane. The assembly of the MUA-Au nanoparticles does not change the Ag-printed IME features, as shown in Fig. 1(e) and (f).

B. Chemiresistive Sensing of Volatile Organic Compounds

The MUA-AuNPs/Ag-IME/PAN/PET paper devices were tested for chemiresistive sensing of various volatile organic compounds (VOCs) under different concentrations. Fig. 2 shows a representative set of sensor response profiles to ethanol and 1-propanl vapors for a MUA-AuNPs/Ag-IME/PAN/PET paper device, as well as a control device fabricated with the same sensing film but on polyimide substrate. The responses to the VOCs are characterized by the resistance increase, which clearly depends on the vapor concentration and the substrate. The response profiles of ethanol and 1-propanol for the sensor on the paper membrane substrate are much higher than that of the sensor on the polyimide substrate, demonstrating the important role of the 3D characteristic of the MUA-AuNPs/Ag-IME/PAN/PET paper device in the sensing properties. Moreover, the response sensitivity, as measured by the slope of sensor response vs. vapor concentration shown in Fig. 2(b) and (d), is different for different vapors. For ethanol it is 6.87×10^{-4}, which is lower than that for 1-propanol, 1.45×10^{-3}.

The response sensitivities to other VOCs, such as methanol, benzene, acetone, hexane, etc. were also determined, showing higher sensitivities for the paper device than those for the polyimide device, as shown in Fig. 3. The paper membrane with 3D-porous structure shows higher sensitivity than the 2D-nonporous polyimide substrate.

The subtle differences in sensitivity for the different VOCs were analyzed in terms of the solubility parameters of the vapor molecules. Total solubility provides a numerical estimate of the degree of interaction between chemicals, and can be a good indication of solubility of the vapor molecules in the sensing film [20]. The expression for total (Hildebrand) solubility parameter (δ_t) is described as follows:

$$\delta_t = \sqrt{\delta_d^2 + \delta_p^2 + \delta_h^2} \quad (1)$$

where

- δ_d is the dispersion solubility parameter
- δ_p is the polar solubility parameter, and
- δ_h is hydrogen bonding solubility parameter.

Theoretically, the total solubility of the vapor molecules is a function of three parameters, including the hydrophobic interactions (i.e., dispersion), polar interaction (i.e., polarity), and hydrogen bonding interaction, as shown in equation 1. Experimentally, the response sensitivity of MUA-linked Au nanoparticle sensing materials on both the paper membrane and the polyimide substrate for alcohols vapors are shown to increase with the decrease of the total solubility. However, the sensitivity increases with increasing the number of carbons in the alcohol chain, as shown in Fig. 3(a). By comparing the sensitivity values for the four different types of VOCs (alcohol, ketone, aromatic, alkane), the sensitivity is shown to decrease with a decrease of the total solubility parameter of VOCs, as shown in Fig. 3(b). The sensitivity of different types of VOCs was clearly dependent on the total

solubility parameter. However, for the same type of VOCs, such as alcohols, the size of the molecule or the number of carbon in the chain is shown to contribute significantly to the sensitivity, demonstrating the important roles of hydrophobicity and polarity. The changes of these two solubility parameters are due to the increased size of alcohol molecules, which increases the relative amount of vapor molecules being adsorbed in the sensing film. As a result, it

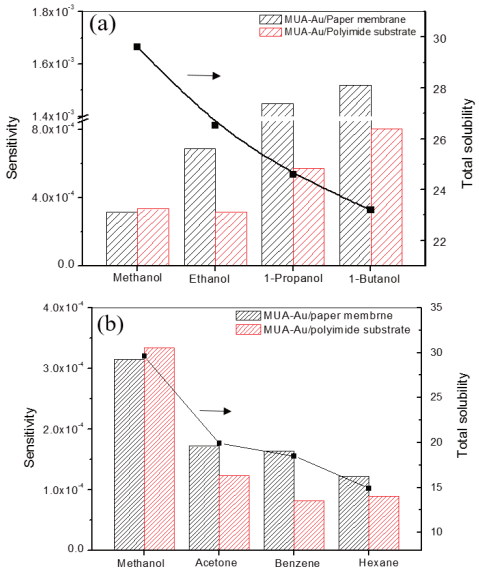

Figure 3. Sensitivity for VOCs of a MUA-linked Au nanoparticle thin film on PAN/PET paper membrane (black) based Ag IME. Sensitivity of Ag IME on polyimide substrate with MUA-linked Au nanoparticle thin film (red) are included for comparison. (a) The sensitivity and total solubility parameters for alcohol vapors as a function of the number of carbons in the alcohol chain. (b) The sensitivity and total solubility parameters for four types of VOCs (alcohol, ketone, aromatic and alkane). The black curve indicates the total solubility parameters for the VOCs.

increases the interparticle distance of nanoparticles in the nanocomposite film, thus increasing the electrical resistance of the chemieresistor.

Note that for the two-layer paper membrane (PAN/PET) the PAN has a pore-diameter of 150±10nm while the PET has a pore-diameter of 20μm. In order to investigate whether PET has the contribution to the sensitivity of VOCs, the PAN layer was peeled off so that PAN and PAN/PET coupled with MUA-linked nanoparticles on Ag printed IME could be tested as sensing materials individually. Fig. 4 shows a set of data for the comparison of the response sensitivities to different VOCs. In addition to showing higher response sensitivities to the polar vapor molecules than those to the non-polar ones, the paper membrane with only PAN layer revealed a sensitivity to the VOCs similar to that of the two layer paper membrane (PAN/PET). This finding suggests that the PET substrate plays only a minor role in the sensing response characteristic.

C. *Evaluation Board Testing*

The printed chemieresestive sensor was connected to a TI CC2650 microcontroller evaluation module to sense the change in resistance response to chemical exposure, using the voltage divider setup described previously. Using this setup, a change in voltage could be detected to signal the change in response to vapors. To demonstrate the viability of this evaluation module, vapors from VOC chemicals or human breath were tested. One example of the testing setup

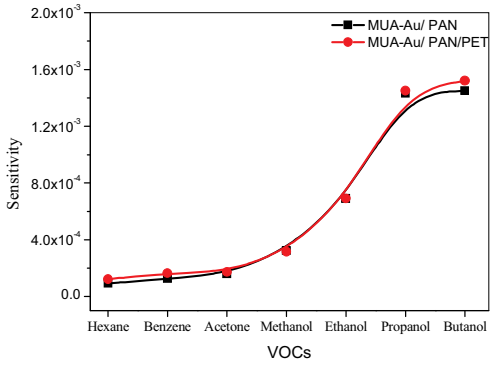

Figure 4. Response sensitivity to different VOCs for a MUA-linked Au nanoparticle thin film as sensing materials on PAN (black) in comparison with that for PAN/PET (red) paper membrane.

is shown in Fig. 5 for a carbon printed IME device on the paper (PAN/PET) with electronics, which include the evaluation module, battery, sensor and computer, shown in Fig. 5(a). A sensor device with MUA-linked Au nanoparticle sensing film was tested with this platform, as shown in Fig. 5(b).

This setup was used for monitoring exposure of the sensor device to acetone vapor in air under ambient conditions. A typical set of sensor response profiles in response to repetitive exposures to acetone vapor in air is shown in Fig. 6, showing largely reproducible response amplitudes. The sensor experienced an increase in resistance as a result of the adsorption of acetone mixed in the ambient air, which causes the voltage observed by the evaluation module to decrease. The observation of the negative response profile was not surprising considering the contributions of the interparticle dielectric medium properties, and the charge hopping conduction mechanism it affects, and the IME parameters to the changes of the electrical conductivity of the sensing film. In comparison with the Ag-ink printed IME devices (printed gap: 140μm), the carbon-printed IME devices might be different in terms of the dispersion of carbon ink in the paper substrate

(printed gap: 40μm), causing subtle differences in actual

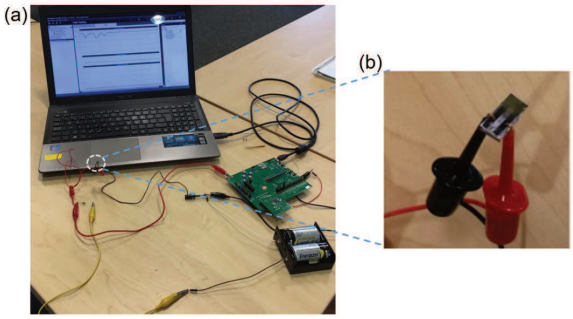

Figure 5. (a) Photo showing the chemiresistor test for integration with microcontroller evaluation module, computer, battery, and paper-based sensor. (b) Photo showing a printed carbon IME on PAN/PET paper with MUA-linked Au nanoparticle thin film.

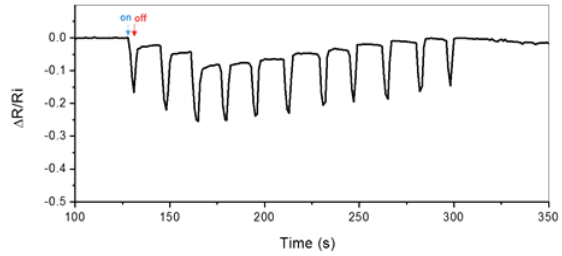

Figure 6. An example set of response profile for multiple acetone vapor exposures on the paper-based sensor with a MUA-linked Au nanoparticle thin film.

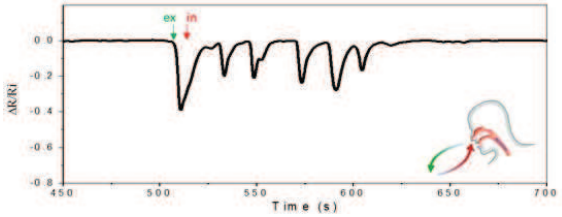

Figure 7. Response of a MUA-linked Au nanoparticle thin film on carbon printed IME to human breathing in terms ofexhale and inhale cycles. Insert: illustration of breathing with exhale (green arrow) and inhale (red arrow) circles.

microelectrode gap, length, and thickness. As shown in previous reports [21], the opposite response profiles were observed for mixtures of acetone and water vapors with IME devices of different microelectrode spacing, where a larger microelectrode spacing showed positive response profile whereas a smaller microelectrode spacing exhibited a negative response profile. An in-depth understanding of the correlation of the response profiles with these parameters of printed IME devices on membrane-type paper substrate is part of on-going investigations.

Importantly, the preliminary result shows that the response is reversible upon turning the vapor flow on and off, and no change was observed when only ambient air was flowed. In view of the increasing evidence showing that acetone is an important biomarker from the breath for diabetes [22], the result demonstrates the viability of the sensor platform for use in a breath sensor monitoring diabetes patients.

We also tested the sensor platform for monitoring the human breathing characteristics in general. Fig. 7 shows a representative set of response profiles for the sensor device in response to multiple exhale and inhale cycles. While there are many types of VOCs, CO_2 and moisture (H_2O) in human breath, which have been a focus of studies of breath sensors [23], the observation of the largely-similar response profile reflecting the breathing pattern supports the viability of developing the sensor as a potential portable or wearable sensor for monitoring human performance in terms of exhale and inhale characteristics. Note that the observation of the negative response profiles indicates that the adsorption of water moisture in the sensing film, causing a change in the dielectric medium properties, is the dominant factor for the electrical response characteristic.

The above preliminary findings have demonstrated the viability of building up to an integrated, paper based flexible sensor on the platform of a TI CC2650 evaluation module. The initial test results support the feasibility of using these paper based sensors with the existing HPM device, where the sensor could be connected to the existing thermistor circuitry. Further integrations in terms of the kind of materials and techniques that will be needed to support it is part of on-going work, which would involve attaching a sensor to an actual HPM with some slight modifications.

D. Integration with a Flexible Sensor Module

The attachment of a printed paper sensor would be fairly straightforward on the existing HPM. As shown in the evaluation board demo, the existing thermistor infrastructure can be used, at least initially. The HPM is currently fabricated with a 660kΩ resistor for the voltage divider used in the thermistor circuit, and this is not ideal given that the evaluation board tests found that a 1MΩ resistor worked well. However, this resistor can be changed, if needed. Additionally, this resistor can eventually be printed as part of the sensor element. It could keep the ratios of resistance in the resistor and sensing element similar, negating changes in response to nuisance factors, while allowing changes only to sensing interactions. The contacts located on the sensor side of the HPM can be connected to paper sensor using a conductive adhesive, which can provide both mechanical and electrical contact to the paper sensor and HPM, as shown in Fig. 8(b). This arrangement would allow the paper sensor to be in conformal contact to the body, in the same way the designed thermistor is, and allow sensing of sweat or vapors that exude from the skin.

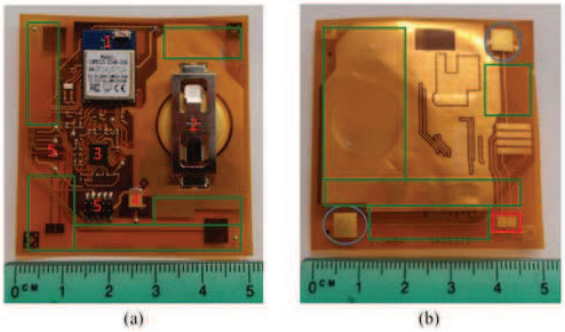

Figure 8. Photographs of the HPM patch component (a) and sensor (b) sides. The component side shows areas that could be used for sensors placement in green boxes. Key components are marked with numbers 1: Microprocessor and Bluetooth radio chip 2: Battery holder 3: Signal conditioning chip for ECG 4: Capacitor for chip power smoothing. 5: Contact points for test and programming. The sensor side shows the area for the thermistor boxed in red, the pads for the ECG sensor circled in blue and open areas for future sensor placement boxed in green. The pads in the red box would be where the printed sensor would be epoxied if it is to replace the thermistor.

In choosing an adhesive, we would select one that is non-toxic and robust. Given that metals such as silver tend to degrade and may show toxicity, we would look for a conductive epoxy based on another material, and have seen Master Bond EP75-1 graphite based epoxy as an alternative to test here. This epoxy, while not being as conductive as metal based ones, is still more conductive than the carbon ink used in the printing of the electrodes, and has a cure schedule that is compatible with the HPM and sensor materials, such as a few hours at 65-95°C after drying overnight at room temperature [24].

Another design involves mounting the sensor on the topside of the HPM, as the area above it is free of components. Changes would need to be made in the design and fabrication of the HPM to allow for these contacts to be on the component side of the HPM, but the same technique could be used to attach the paper based sensor there, and these areas are shown in Fig. 8(a). Additionally, a total of 8 channels are available for analog sensing in the electronics of the HPM, and so it would be possible to place more sensors on both sides of the HPM. This design would allow multifactor analysis for the sensing and identification of chemicals.

IV. Summary and Conclusions

In summary, a novel printed nanoparticle chemiresistor sensor on paper was demonstrated. These sensors are shown to be sensitive to a variety of chemicals, with an enhanced response when fabricated on paper as opposed to a conventional polyimide substrate. An attempt was also made to create a fully integrated, flexible, disposable paper based sensor. This is done by leveraging electronic systems and coupling the printed paper electrode to it. An evaluation module test has demonstrated that this sensor is compatible with the electronics used on this system, showing promise for further optimization. A plan for integration is discussed, aiming for the creation of a wireless, flexible sensor module.

From these results, we can conclude that printed paper chemical sensors are effective, creating a low cost alternative to rigid, lithographically fabricated sensor devices. This low-cost disposable sensor is ideal for integration with a disposable hybrid flexible electronics patch. In addition to providing a chemical sensing capability to the patch, the patch provides power to the sensor and the ability to transmit data for logging and analysis, all in a flexible and disposable form.

Acknowledgment

Financial support of this work from SUNY Network of Excellence Fund, and in part from NSF (IIP 1640669), is gratefully acknowledged.

References

[1] A. Pantelopoulos and N. G. Bourbakis, "A Survey on Wearable Sensor-Based Systems for Health Monitoring and Prognosis," IEEE Trans. Syst. Man Cybern. Part C Appl. Rev., vol. 40, no. 1, pp. 1–12, Jan. 2010.

[2] B. Kuswandi, Y. Wicaksono, Jayus, A. Abdullah, L. Y. Heng, and M. Ahmad, "Smart packaging: sensors for monitoring of food quality and safety," Sens. Instrum. Food Qual. Saf., vol. 5, no. 3–4, pp. 137–146, Dec. 2011.

[3] J. Kim, R. Kumar, A. J. Bandodkar, and J. Wang, "Advanced Materials for Printed Wearable Electrochemical Devices: A Review," Adv. Electron. Mater., vol. 3, no. 1, p. n/a-n/a, Jan. 2017.

[4] C. K. Ho, A. Robinson, D. R. Miller, and M. J. Davis, "Overview of sensors and needs for environmental monitoring," Sensors, vol. 5, no. 1, pp. 4–37, 2005.

[5] W. Dungchai, O. Chailapakul, and C. S. Henry, "Electrochemical Detection for Paper-Based Microfluidics," Anal. Chem., vol. 81, no. 14, pp. 5821–5826, Jul. 2009.

[6] A. Arena, N. Donato, G. Saitta, A. Bonavita, G. Rizzo, and G. Neri, "Flexible ethanol sensors on glossy paper substrates operating at room temperature," Sens. Actuators B Chem., vol. 145, no. 1, pp. 488–494, Mar. 2010.

[7] C. Steffens et al., "Low-cost sensors developed on paper by line patterning with graphite and polyaniline coating with supercritical CO2," Synth. Met., vol. 159, no. 21–22, pp. 2329–2332, Nov. 2009.

[8] H. Ma et al., "High-flux thin-film nanofibrous composite ultrafiltration membranes containing cellulose barrier layer," J. Mater. Chem., vol. 20, no. 22, p. 4692, 2010.

[9] N. Kang et al., "Nanoparticle–Nanofibrous Membranes as Scaffolds for Flexible Sweat Sensors," ACS Sens., vol. 1, no. 8, pp. 1060–1069, Aug. 2016.

[10] S. Imani et al., "A wearable chemical–electrophysiological hybrid biosensing system for real-time health and fitness monitoring," Nat. Commun., vol. 7, p. 11650, May 2016.

[11] W. Gao et al., "Fully integrated wearable sensor arrays for multiplexed in situ perspiration analysis," Nature, vol. 529, no. 7587, pp. 509–514, Jan. 2016.

[12] M. Poliks et al., "A Wearable Flexible Hybrid Electronics ECG Monitor," in 2016 IEEE 66th Electronic Components and Technology Conference (ECTC), 2016, pp. 1623–1631.

[13] Y. Khan et al., "Flexible Hybrid Electronics: Direct Interfacing of Soft and Hard Electronics for Wearable Health Monitoring," Adv. Funct. Mater., vol. 26, no. 47, pp. 8764–8775, Dec. 2016.

[14] M. J. Hostetler et al., "Alkanethiolate Gold Cluster Molecules with Core Diameters from 1.5 to 5.2 nm: Core and Monolayer Properties

as a Function of Core Size," Langmuir, vol. 14, no. 1, pp. 17–30, Jan. 1998.

[15] M. M. Maye, W. Zheng, F. L. Leibowitz, N. K. Ly, and C.-J. Zhong, "Heating-Induced Evolution of Thiolate-Encapsulated Gold Nanoparticles: A Strategy for Size and Shape Manipulations," Langmuir, vol. 16, no. 2, pp. 490–497, Jan. 2000.

[16] L. Han et al., "Nanoparticle-structured sensing array materials and pattern recognition for VOC detection," Sens. Actuators B Chem., vol. 106, no. 1, pp. 431–441, Apr. 2005.

[17] WangWang et al., "Array of Molecularly Mediated Thin Film Assemblies of Nanoparticles: Correlation of Vapor Sensing with Interparticle Spatial Properties," J. Am. Chem. Soc., vol. 129, no. 7, pp. 2161–2170, Feb. 2007.

[18] L. Wang et al., "Flexible chemiresistor sensors: thin film assemblies of nanoparticles on a polyethylene terephthalate substrate," J. Mater. Chem., vol. 20, no. 5, pp. 907–915, Jan. 2010.

[24] "EP75-1 Product Information | MasterBond.com." [Online]. Available: http://www.masterbond.com/tds/ep75-1. [Accessed: 17-Feb-2017].

[19] H. Ma et al., "High-flux thin-film nanofibrous composite ultrafiltration membranes containing cellulose barrier layer," J. Mater. Chem., vol. 20, no. 22, p. 4692, 2010.

[20] C. Hansen, Hansen Solubility Parameter: A User's Handbook. Florida: CRC Press, 2000.

[21] J. Luo *et al.*, "Nanoparticle-structured thin film sensor arrays for breath sensing," *Sensors and Actuators B: Chemical*, vol. 161, no. 1, pp. 845–854, Jan. 2012.

[22] A. Prabhakar et al., "Acetone as biomarker for ketosis buildup capability - a study in healthy individuals under combined high fat and starvation diets," Nutr. J., vol. 14, no. 1, Dec. 2015.

[23] F. Güder et al., "Paper-Based Electrical Respiration Sensor," Angew. Chem. Int. Ed., vol. 55, no. 19, pp. 5727–5732, May 2016.